

Photon Long-Range Repulsive Interaction in the Jaynes-Cummings Lattice with Rydberg Atoms

Yuanwei Zhang,^{1,2} Jingtao Fan,¹ J.-Q. Liang,² Jie Ma,¹ Gang Chen,^{1,*} Suotang Jia,¹ and Franco Nori^{3,4}

¹State Key Laboratory of Quantum Optics and Quantum Optics Devices,
Institute of Laser Spectroscopy, Shanxi University, Taiyuan 030006, P. R. China

²Institute of Theoretical Physics, Shanxi University, Taiyuan 030006, P. R. China

³Center for Emergent Matter Science, RIKEN, Wako-shi, Saitama 351-0198, Japan

⁴Physics Department, University of Michigan, Ann Arbor, Michigan 48109-1040, USA

We propose how to realize a strong photon long-range repulsive interaction by controlling the van der Waals repulsive force between Rydberg atoms located in different cavities in extended Jaynes-Cummings-Hubbard lattices. We find that this photon long-range repulsive interaction can generate complex quantum phases, some of which have no analogy in condensed-matter and atomic physics. For example, without photon hopping, a photon devil's staircase induced by the breaking of long-range translation symmetry can emerge. If photon hopping occurs, we predict a photon-floating solid phase, due to the motion of particle- and hole-like defects. More importantly, for a large chemical potential in the resonant case, the photon hopping can be frozen even if the hopping term exists. We call this new phase the photon-frozen solid phase. In experiments, these predicted phases could be detected by measuring the number of polaritons via resonance fluorescence.

PACS numbers: 42.50.Pq, 71.36.+c, 05.30.Rt

Introduction.—The realization of coherent interactions between individual photons is a long-standing goal in science and engineering, because strong photon-photon interactions play an essential role in achieving photon quantum information processing [1] as well as in exploring exotic many-body phenomena of light [2, 3]. In contrast to electrons, interacting directly via Coulomb repulsion, the photon-photon interactions must be mediated by matter [4]. Recently, the on-site photon-blocked effect [5] has been studied in an array of coupled cavities with each cavity interacting with a two-level atom, described by the Jaynes-Cummings-Hubbard (JCH) model [6]. By varying the photon hopping, quantum simulations [3] have studied complex many-body phenomena in condensed-matter and atomic physics, such as the superfluid-Mott-insulator transition [7–17], quantum magnetic dynamics [18], glassy phases [19], solid [20, 21] and supersolid [22] phases, and the fractional quantum Hall effect [23, 24].

In this work, we propose how to realize a photon long-range repulsive interaction (PLRRI) by controlling the van der Waals force between Rydberg atoms located in different cavities in extended JCH lattices. Under current experimental parameters, the PLRRI can reach the strong-coupling regime, and thus generate complex quantum phases, some of which have no analogy in condensed-matter and atomic physics. For example, without photon hopping, the breaking of long-range translation symmetry induces a complex solid structure, i.e., a photon devil's staircase. In a “devil's staircase”, any two different rational states are separated by many states. If photon hopping exists, a photon-floating solid phase is predicted, due to the motion of particle- and hole-like defects. More importantly, for a large chemical potential

in the resonant case, photon hopping can be frozen even if the hopping term exists. We denote this new phase the photon-frozen solid phase. In experiments, these predicted phases could be detected by measuring the number of polaritons via resonance fluorescence [25].

Model.—The Hamiltonian for our considered 1D JCH model, with the van der Waals interaction between Rydberg atoms located in different cavities, is [26]

$$H = H_{\text{JC}} + H_{\text{HOP}} + H_{\text{V}} - \mu N. \quad (1)$$

Here, $H_{\text{JC}} = \sum_i [\omega a_i^\dagger a_i + \epsilon |R\rangle_i \langle R|_i + g(a_i^\dagger |G\rangle_i \langle R|_i + a_i |R\rangle_i \langle G|_i)]$ describes the interaction between the photons and the effective two-level Rydberg atoms for all cavities, where ω is the effective photon frequency, ϵ is the effective transition frequency of the two-level Rydberg atoms, $|G\rangle_i = |g_1, \dots, g_{N_R}\rangle_i$ is the collective ground state, $|R\rangle_i = \sum_f^{N_R} |r_f\rangle \langle g_f| \otimes |G\rangle_i / \sqrt{N_R}$ is the collective state with only a single Rydberg excitation, g is the collective atom-photon interaction strength, and N_R is the number of Rydberg atoms at each cavity. $H_{\text{HOP}} = -\kappa \sum_i (a_i^\dagger a_{i+1} + a_{i+1}^\dagger a_i)$ governs the photon hopping between two adjacent cavities, where κ is the hopping amplitude. The long-range van der Waals interaction is $H_{\text{V}} = \sum_{ij} V(i-j) |R\rangle_i \langle R|_i \otimes |R\rangle_j \langle R|_j / 2$, where $V(i-j) = C_6 / (x_i - x_j)^6$, with $C_6 (> 0)$ being the van der Waals coefficient and x_i being the position of the i th cavity [27]. Hereafter, we use the nearest-neighbor interaction to represent the entire van der Waals interaction, i.e., $V \equiv V_1$, because $V_2 = V_1/2^6$, $V_3 = V_1/3^6$, and $V_4 = V_1/4^6, \dots$. The chemical potential μ is the Lagrange multiplier, and the total number of polaritons is given by $N = \sum_i n_i = \sum_i (a_i^\dagger a_i + |R\rangle_i \langle R|_i)$. In this work, we mainly study the case of strong atom-photon interaction and ultrahigh-finesse cavities. In this case, we

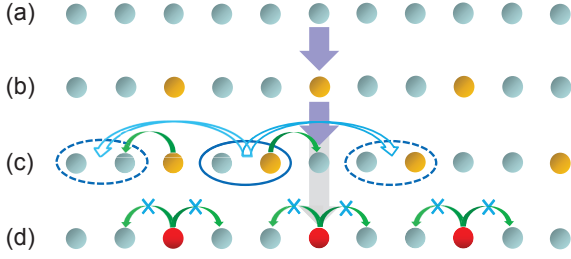


FIG. 1: (Color online) Photon distribution of each cavity for different effective strengths of the van der Waals interaction V , when increasing the chemical potential μ . (a-b) $\kappa = 0$ with a weak V , (c) $\kappa \neq 0$ with a weak V , and (d) $\kappa \neq 0$ with a large μ and a strong V . The vacuum state $|0\rangle$ is denoted by light blue disks, and the photon excitation state $|\tilde{1}\rangle$ is shown in orange. (a) In the initial state, every cavity is in its vacuum state. (b) By increasing μ , some cavities are excited, and rich photon solid phases, whose periods depend strongly on the magnitude of the PLRRI, can emerge. As an example, here we plot a photon solid phase with a period of 3 sites ($\dots|0\rangle|0\rangle|\tilde{1}\rangle|0\rangle|0\rangle|\tilde{1}\rangle\dots$). (c) Melting of this photon solid phase. A particle-like defect with the unit cell $|0\rangle|\tilde{1}\rangle$ is shown inside the blue solid elliptic curve. When a photon on the edge of the defect hops one site, this defect will move three sites (the new possible positions are labeled by dashed ellipses). (d) Plot of a photon-frozen solid phase, which is composed of the $|0\rangle$ and $|\tilde{2}\rangle$ (red color) states.

can ignore the loss terms since they only change slightly the phase boundaries [28, 29].

PLRRI.—We first realize the PLRRI in terms of H_V . We begin to address the simplest case, $\kappa = V = 0$, in which (S7) reduces to $H_S = H_{JC} - \mu N$. The eigenstates (eigenvalues) of H_S are given by $|0-\rangle_i \equiv |0, G\rangle_i$ ($E_0 = 0$), for $n = 0$, and $|n+\rangle_i = \sin\theta_n |n, G\rangle_i + \cos\theta_n |n-1, R\rangle_i$ and $|n-\rangle_i = \cos\theta_n |n, G\rangle_i - \sin\theta_n |n-1, R\rangle_i$ ($E_{n\pm}^\mu = n(\omega - \mu) + \delta/2 \pm \sqrt{(\delta/2)^2 + ng^2}$), for $n \geq 1$, where the angle $2\theta_n = \arctan(2g\sqrt{n}/\delta)$ and the detuning $\delta = \omega - \epsilon$. Since here we investigate the lower-energy behavior, only the lower polariton branch $|n-\rangle$ is considered [6]. Thus, H_S is rewritten as $H_S = \sum_i \sum_n [n(\omega - \mu) + \delta/2] |\tilde{n}\rangle_i \langle \tilde{n}|_i - \sum_i \sum_n \sqrt{(\delta/2)^2 + ng^2} |\tilde{n}\rangle_i \langle \tilde{n}|_i$, where $|\tilde{n}\rangle_i = |n-\rangle_i$. The second term of H_S leads to an even distribution of polaritons, which provides an effective on-site repulsive interaction between photons [6]. When $\kappa \ll g$, the rotating-wave approximation is reasonable, and thus the hopping term becomes $H_{HOP} = -\kappa \sum_n \sum_i t_{n,m} (|\tilde{m}\rangle_i \langle \tilde{n}|_i \otimes |\tilde{n}\rangle_{i+1} \langle \tilde{m}|_{i+1} + \text{H.c.})$, where $t_{n,m} = (\sqrt{m} \cos\theta_n \cos\theta_m + \sqrt{n} \sin\theta_n \sin\theta_m)^2$ and $|\tilde{m}\rangle_i = |m-\rangle_i$, with $m = n + 1$. In addition, since the upper polariton branch $|n+\rangle$ has the higher probability of Rydberg excitation (stronger repulsive interaction), we also only consider the projection of the van der Waals interaction into the lower polariton branch $|n-\rangle$. Thus,

the corresponding Hamiltonian becomes

$$H_V^{n,n'} = \sum_{ij} \sum_{n,n'>0} \frac{J_{n,n'}(i-j)}{2} |\tilde{n}\rangle_i \langle \tilde{n}|_i \otimes |\tilde{n}'\rangle_j \langle \tilde{n}'|_j, \quad (2)$$

where $J_{n,n'}(i-j) = V(i-j) \langle \tilde{n}|_i \langle \tilde{n}'|_j (|R\rangle_i \langle R|_i \otimes |R\rangle_j \langle R|_j) |\tilde{n}\rangle_j \langle \tilde{n}'|_i = V(i-j) \sin^2\theta_n \sin^2\theta_{n'}$ is the effective interaction strength. Since $V(i-j) > 0$, Eq.(2) demonstrates explicitly that the van der Waals interaction generates an effective PLRRI, which leads to non-trivial quantum phases exhibiting photon solid states, as will be shown below.

Quantum phases and phase diagrams.— We now investigate quantum phases and phase diagrams by perturbation theory and a mapping into an effective Hamiltonian. For instance, when μ is weak, the high occupancy states ($n > 1$) of (S7) is not considered. In such case, we rewrite (S7) in a reduced Hilbert space, with $n = 0, 1$, as $H_{\text{eff}} = -J_\perp \sum_i (|\tilde{1}\rangle_i \langle 0|_i \otimes |0\rangle_{i+1} \langle \tilde{1}|_{i+1} + \text{H.c.}) + \sum_{ij} J_\parallel (i-j) |\tilde{1}\rangle_i \langle \tilde{1}|_i \otimes |\tilde{1}\rangle_j \langle \tilde{1}|_j / 2 + E_{1-}^\mu \sum_i |\tilde{1}\rangle_i \langle \tilde{1}|_i$, where $J_\perp = \kappa \cos^2\theta_1$, $J_\parallel(i-j) = J_{1,1}(i-j)$, and $E_{1-}^\mu = \omega - \mu + \delta/2 - \sqrt{(\delta/2)^2 + g^2}$ is the single-particle energy of $|\tilde{1}\rangle$ state.

We first consider the case without the photon hopping ($\kappa = 0$). At $t = 0$, we assume that every cavity is in its vacuum state; see Fig.1(a). When increasing μ , photons in some cavities can be excited (without the PLRRI, all cavities are excited identically [6]), due to existence of the PLRRI, and some $|\tilde{1}\rangle$ states emerges; see Fig.1(b). The corresponding critical point is given by $(\mu_{c0} - \omega)/g = \delta/2g - \sqrt{1 + (\delta/2g)^2}$, derived from $E_{1-}^\mu(\mu_{c0}) = 0$. Since the $|\tilde{1}\rangle$ states are generated one by one and deviate from each other, the system exhibits photon solid states, which are mainly governed by different filling factors $\rho = p/q$ (≤ 1), with p and q being both integers. In order to quantitatively figure out ρ , we introduce X_i^0 and X_i^l , where X_i^0 is the position of the i th $|\tilde{1}\rangle$ state and X_i^l is the distance to the l th next $|\tilde{1}\rangle$ state, satisfying $X_i^l = X_{i+l}^0 - X_i^0$. When the ground-state energy is minimized for all sites, we have

$$X_i^l = r_l \quad \text{or} \quad r_l + 1, \quad (3)$$

where $r_l < l/\rho < r_l + 1$ and satisfy the following relation: [30, 31]

$$\sum_i X_i^l = lN. \quad (4)$$

For a given filling state, the repulsive interaction energy of the $|\tilde{1}\rangle$ states can be estimated by applying the relations in Eqs.(3, 4) to H_{eff} . Moreover, the corresponding phases are stable if it costs energy to add or remove a particle and rearrange the structure.

We define the photon solid state, with the filling factor ρ , as $|c\rangle_q$. If we add one $|\tilde{1}\rangle$ state, $|c\rangle_q$ becomes $|p\rangle_q$ and

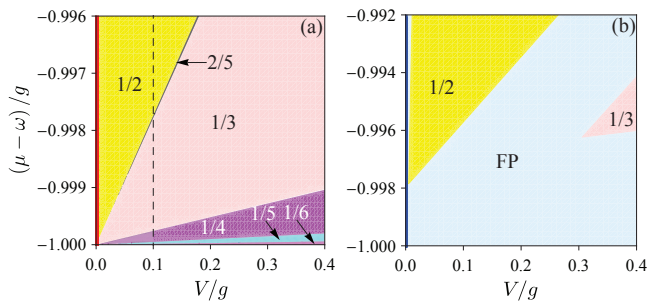


FIG. 2: (Color online) The filling factor $\rho = p/q$ as a function of the chemical potential μ and the effective strength of the van der Waals interaction V , for (a) $\kappa/g = 0$ and (b) $\kappa/g = 0.001$, when $\delta = 0$. In (b), FP denotes the photon-floating solid phase.

the $|\tilde{1}\rangle$ states are crowded. To minimize the repulsive energy, the summation of distances between the $|\tilde{1}\rangle$ states must be minimum. Thus, the most likely rearrangement structure is that some pairs of the adjacent $|\tilde{1}\rangle$ states are shortened by one site [5, 30]. Since the relations in Eqs.(3, 4) must still hold, r_l $|\tilde{1}\rangle$ state pairs with $X_i^l = (r_l + 1)$ must be replaced by $(r_l + 1)$ $|\tilde{1}\rangle$ state pairs with $X_i^l = r_l$. In addition, at the phase-transition point, there is no energy gap between $|c\rangle_q$ and $|p\rangle_q$, i.e., $E(|c\rangle_q) = E(|p\rangle_q)$ [5], and the critical point is thus obtained by $\mu_\rho^0(p) = \omega + \delta/2 - \sqrt{(\delta/2)^2 + g^2} + \sum_{k=1, k \neq fp}^\infty [(r_k + 1)J_{||}(r_k) - r_k J_{||}(r_k + 1)] + \sum_{k=1}^\infty [kqJ_{||}(kq - 1) - (kq - 1)J_{||}(kq)]$, where f is any integer [26]. Similarly, if we remove one $|\tilde{1}\rangle$ state, $|c\rangle_q$ turns into $|h\rangle_q$, and the corresponding critical point is given by $\mu_\rho^0(h) = \omega + \delta/2 - \sqrt{(\delta/2)^2 + g^2} + \sum_{k=1, k \neq fp}^\infty [(r_k + 1)J_{||}(r_k) - r_k J_{||}(r_k + 1)] + \sum_{k=1}^\infty [(kq + 1)J_{||}(kq) - kqJ_{||}(kq + 1)]$ [26]. In terms of the obtained $\mu_\rho^0(p)$ and $\mu_\rho^0(h)$, the stability interval, $\Delta\mu_\rho = \mu_\rho^0(p) - \mu_\rho^0(h)$, is evaluated as $\Delta\mu_\rho = \sum_{k=1}^\infty kqJ_{||}(kq + 1) + kqJ_{||}(kq - 1) - 2kqJ_{||}(kq)$. The expression for $\Delta\mu_\rho$ shows that the stability interval is only dependent on q , and moreover, decreases rapidly when increasing q . This means that the photon solid phases with $p = 1$, i.e., $\rho = 1/q = 1/2, 1/3, 1/4, \dots$, are more likely to be observed. Below, we mainly address these phases.

In Fig.2(a), we plot ρ as a function of μ and V in terms of $\mu_\rho^0(p)$ and $\mu_\rho^0(h)$. For $V = 0$, $\rho = 1$, as expected [see the red solid line in Fig.2(a)]. However, the results for finite V [for example, $V = 0.1g$; see the black dashed line in Fig.2(a)] are very interesting. When increasing μ , ρ is not a constant, but varies jumpily from $1/6, 1/5, 1/2, 1/4, 1/3, 2/5$, to $1/2$. The reason is that when increasing μ , E_{1-}^μ decreases, and excitation of the cavities is thus favorable. This behavior clearly shows a devil's staircase [5, 33]. Moreover, this devil's stair-

case can be detected experimentally by the mean-photon number $\langle a^\dagger a \rangle / L$ since $\langle a^\dagger a \rangle / L = \rho/2$, and thus here called by the photon devil's staircase. On contrary, when increasing V , ρ varies jumpily from high to low because the PLRRI prevents the photon excitation. Recently, the photon nearest-neighbor interaction was studied and a photon solid state was predicted [20]. In that case, the Z_2 symmetry, translation by one site, has been broken. Here the PLRRL generates a long-range translation symmetry, whose breaking induces the photon devil's staircase. Moreover, it leads to another non-trivial phases when the photon hopping exists.

Notice that between the adjacent photon solid phases, with $\rho = 1/q$ and $\rho = 1/(q \mp 1)$, respectively, there are many transition states which have different numbers of defects. Here we define the pairs of the $|\tilde{1}\rangle$ states with shorter (longer) distance as a particle- (hole-) like defect structure. Since these states have very small stability intervals, they are also hard to be observed when $\kappa = 0$, and thus not plotted in Fig.1(b). However, when $\kappa \neq 0$, they play an important role for the ground-state properties, because of the motion of the defects; see Fig.1(c). Especially, when the hopping energy is negative, the states with defects may be more stable than the adjacent photon solid states. As a result, the photon solid phases are melted and a photon-floating solid phase [34] can emerge. Generally, we cannot discuss completely this process. However, in the region closed to the phase-transition point, the repulsive interaction between the defects makes only one defect exist. Thus, the phase boundary can be estimated by comparing the energy of the photon solid state $|c\rangle_q$ with that of the state with one defect. Using a perturbation method, the phase boundaries are given by [26]

$$\mu_\rho^{\text{up}} = \mu_\rho^0(p) - 2qJ_\perp, \quad \mu_\rho^{\text{down}} = \mu_\rho^0(h) + 2qJ_\perp. \quad (5)$$

Equation (5) shows that the hopping energies of the defects reduce the regions where the photon solid phases exist, because $\mu_\rho^{\text{up}} - \mu_\rho^{\text{down}} = \Delta\mu_\rho - 4qJ_\perp$. In particular, when $q \geq \Delta\mu_\rho / (4J_\perp)$, $\mu_\rho^{\text{up}} \leq \mu_\rho^{\text{down}}$, and thus the energy bands of the particle- and hole-like defect states are crossed and the photon solid phases cannot exist. This is the reason why only the photon solid phases, with $\rho = 1/2$ and $\rho = 1/3$, can emerge in Fig.2(b). From Fig.2(b) we also see that the regions where the photon solid phases exist are very small, and are melted in a smaller κ ($\kappa/g = 0.001$). This implies that the hopping term can be treated as a perturbation. So the results of phase boundaries in Eq.(5) are reasonable. Strictly speaking, in the photon-floating solid phase, the total number of the $|\tilde{1}\rangle$ states is sensitive to the fluctuation of parameters, and ρ or $\langle a^\dagger a \rangle / L$ is hard to calculate. The quantum Monte Carlo method [35] is a suitable method to solve this problem. When $V = 0$, the photon-floating solid phase disappears [see the blue line in Fig.2(b)].

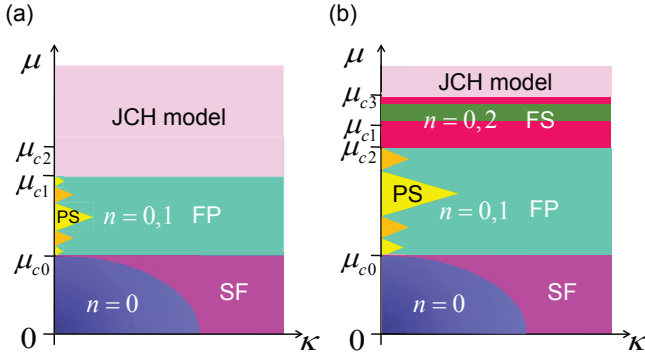


FIG. 3: (Color online) Schematics of the ground-state phase diagrams for (a) $\mu_{c1} < \mu_{c2}$ and (b) $\mu_{c1} > \mu_{c2}$, when $\delta = 0$. In (a) and (b), all cavities can be excited, when $\mu > \mu_{c1}$ and $\mu > \mu_{c3}$, respectively. Here, SF, PS, FP, and FS denote the following phases: superfluid, photon solid, photon-floating solid, and photon-frozen solid, respectively. This figure is not to scale.

Finally, we address the case of strong μ , in which the higher photon occupancy states in some cavities can occur, and moreover, the single-particle energy of the $|\tilde{2}\rangle$ state, E_{2-}^{μ} , is close to that of the $|\tilde{1}\rangle$ state, E_{1-}^{μ} , (here we omit the case $n > 2$). In this case, there exists three kinds of repulsive interactions: $|\tilde{1}\rangle$ to $|\tilde{1}\rangle$ states, $|\tilde{2}\rangle$ to $|\tilde{2}\rangle$ states, and $|\tilde{1}\rangle$ to $|\tilde{2}\rangle$ states. Moreover, the photon hopping has two channels, from $|0\rangle$ to $|\tilde{1}\rangle$ states and $|\tilde{1}\rangle$ to $|\tilde{2}\rangle$ states. This case is very complex. However, in the resonance case ($\delta = 0$), $\sin^2 \theta_n = 1/2$, and $H_V^{n,n'}$ is thus independent on n . This indicates that the photon numbers of the excited cavities are determined only by E_{1-}^{μ} and E_{2-}^{μ} . When the PLRRI is not sufficiently strong, the lattice can be fully filled in the weak μ region. In this region, $E_{2-}^{\mu} > E_{1-}^{\mu}$, and the ground state, still governed by H_{eff} , is thus composed of the $|0\rangle$ and $|\tilde{1}\rangle$ states. By increasing μ , ρ increases from 0 and reaches 1. Further increasing μ , all cavities can be excited with uniform photon numbers, which is similar to that of the standard JCH model; see Fig.3(a).

However, there is a non-trivial case for a strong PLRRI; see Fig.3(b). In such case, the photon solid phases can exist in the strong μ region. But we cannot ensure that the lattice is fully filled by the $|\tilde{1}\rangle$ states due to inversion of E_{1-}^{μ} and E_{2-}^{μ} . This process can be determined by comparing $\mu_{c1} \approx \omega - g + 1.0175V$, obtained by making $\rho = 1$ in $\mu_p^0(h)$, with the other critical point $\mu_{c2} \approx \omega + 0.414g$ (the degenerate point of $E_{1-}^{\mu_{c2}}$ and $E_{2-}^{\mu_{c2}}$). When $V > 0.576g$, $\mu_{c1} > \mu_{c2}$, and there is a transition from the $|\tilde{1}\rangle$ to $|\tilde{2}\rangle$ states in the excited cavities. Thus, this transition induces a new crystalline configuration, which is composed of the $|0\rangle$ and $|\tilde{2}\rangle$ states. The corresponding low-energy behavior is governed by a new effective Hamiltonian $H'_{\text{eff}} =$

$\sum_{ij} J_{\parallel} (i-j) |\tilde{2}\rangle_i \langle \tilde{2}|_i \otimes |\tilde{2}\rangle_j \langle \tilde{2}|_j / 2 + E_{2-}^{\mu} \sum_i |\tilde{2}\rangle_i \langle \tilde{2}|_i$, where $J_{\parallel} (i-j) = J_{2,2} (i-j) = J_{1,1} (i-j)$ and $E_{2-}^{\mu} = 2(\omega - \mu) - \sqrt{2}g$. Since $\langle 0|_{i+1} \langle \tilde{2}|_i (a_i^{\dagger} a_{i+1}) |0\rangle_i |\tilde{2}\rangle_{i+1} = 0$, the photon hopping is always frozen even if κ exists. We call the corresponding phase as the photon-frozen solid phase. In this phase, the fraction filling structure of the $|\tilde{2}\rangle$ states is robust, i.e., it is not easily destroyed by the photon hopping. In terms of H'_{eff} , when further increasing μ to satisfy $\mu > \mu_{c3} \approx (2\omega - \sqrt{2}g + 1.0175V)/2$, the lattice can be fully filled by the $|\tilde{2}\rangle$ states; see Fig.3(b).

Conclusions.—In summary, we have achieved a strong PLRRI by controlling the van der Waals interaction of Rydberg atoms located in different cavities in extended JCH lattices, and then predicted novel quantum phases, some of which have no analogy in condensed-matter and atomic physics. Due to the rapid development of experiments with ultrahigh- Q coupled nanocavities [36] and Rydberg atoms [27], our proposal might help to explore rich many-body phenomena of light and quantum nonlinear optics, as well as potential applications to quantum information and computing.

Acknowledgements.—This work is supported in part by the 973 program under Grant No.2012CB921603; the NNSFC under Grant Nos.11422433, 11434007 and 61275211; the PCSIRT under Grant No. IRT13076; the NCET under Grant No.13-0882; the FANEDD under Grant No.201316; the OIT under Grant No.2013804; OYTPSP; and SSCC. FN is partially supported by the RIKEN iTHES Project, MURI Center for Dynamic Magneto-Optics, and a Grant-in-Aid for Scientific Research (S).

* Corresponding author: chengang971@163.com

- [1] T. E. Northup and R. Blatt, Nat. Photon. **8**, 356 (2014).
- [2] I. Carusotto and C. Ciuti, Rev. Mod. Phys. **85**, 299 (2013).
- [3] I. M. Georgescu, S. Ashhab, and F. Nori, Rev. Mod. Phys. **86**, 153 (2014).
- [4] D. E. Chang, V. Vuletić, and M. D. Lukin, Nat. Photon. **8**, 685 (2014).
- [5] K. M. Birnbaum, A. Boca, R. Miller, A. D. Boozer, T. E. Northup, and H. J. Kimble, Nature (London) **436**, 87 (2005).
- [6] M. J. Hartmann, F. G. S. L. Brandão, and M. B. Plenio, Laser Photon. Rev. **2**, 527 (2008).
- [7] A. D. Greentree, C. Tahan, J. H. Cole, and L. C. L. Hollenberg, Nat. Phys. **2**, 856 (2006).
- [8] M. J. Hartmann, F. G. S. L. Brandão, and M. B. Plenio, Nat. Phys. **2**, 849 (2006).
- [9] D. G. Angelakis, M. F. Santos, and S. Bose, Phys. Rev. A **76**, 031805 (2007).
- [10] M. J. Hartmann and M. B. Plenio, Phys. Rev. Lett. **99**, 103601 (2007).
- [11] M. Aichhorn, M. Hohenadler, C. Tahan, and P. B. Littlewood, Phys. Rev. Lett. **100**, 216401 (2008).
- [12] N. Na, S. Utsunomiya, L. Tian, and Y. Yamamoto, Phys. Rev. A **77**, 031803 (2008).

- [13] S. Schmidt and G. Blatter, *Phys. Rev. Lett.* **103**, 086403 (2009).
- [14] J. Koch and K. L. Hur, *Phys. Rev. A* **80**, 023811 (2009).
- [15] A. Tomadin, V. Giovannetti, R. Fazio, D. Gerace, I. Carusotto, H. E. Türeci, and A. Imamoglu, *Phys. Rev. A* **81**, 061801(R) (2010).
- [16] M. Schiró, M. Bordyuh, B. Öztop, and H. E. Türeci, *Phys. Rev. Lett.* **109**, 053601 (2012).
- [17] K. Seo and L. Tian, arXiv:1408.2304.
- [18] A. -C. Ji, X. C. Xie, and W. M. Liu, *Phys. Rev. Lett.* **99**, 183602 (2007).
- [19] D. Rossini and R. Fazio, *Phys. Rev. Lett.* **99**, 186401 (2007).
- [20] J. Jin, D. Rossini, R. Fazio, M. Leib, and M. J. Hartmann, *Phys. Rev. Lett.* **110**, 163605 (2013).
- [21] J. Jin, D. Rossini, M. Leib, M. J. Hartmann, and R. Fazio, *Phys. Rev. A* **90**, 023827 (2014).
- [22] B. Bujnowski, A. L. C. Hayward, J. Cole, and A. M. Martin, arXiv: 1310.4548.
- [23] A. L. C. Hayward, A. M. Martin, and A. D. Greentree, *Phys. Rev. Lett.* **108**, 223602 (2012).
- [24] M. Hafezi, M. D Lukin, and J. M Taylor, *New J. Phys.* **15** 063001 (2013).
- [25] K. Toyoda, Y. Matsuno, A. Noguchi, S. Haze, and S. Urabe, *Phys. Rev. Lett.* **111**, 160501 (2013).
- [26] See Supplementary Material for detailed discussions.
- [27] M. Saffman, T. G. Walker, and K. Mølmer, *Rev. Mod. Phys.* **82**, 2313 (2010).
- [28] Y. Zhang, L. Yu, J. -Q. Liang, G. Chen, S. Jia, and F. Nori, *Sci. Rep.* **4**, 4083 (2014).
- [29] J. Ruiz-Rivas, E. del Valle, C. Gies, P. Gartner, M. J. Hartmann, arXiv:1401.5776.
- [30] J. Hubbard, *Phys. Rev. B* **17**, 494 (1978).
- [31] V. L. Pokrovsky and G. V. Uimin, *J. Phys. C* **11**, 3535 (1978).
- [32] P. Bak and R. Bruinsma, *Phys. Rev. Lett.* **49**, 249 (1982).
- [33] C. Reichhardt and F. Nori, *Phys. Rev. Lett.* **82**, 414 (1999).
- [34] P. Fendley, K. Sengupta, and S. Sachdev, *Phys. Rev. B* **69**, 075106 (2004).
- [35] J. Zhao, A.W. Sandvik, and K. Ueda, arXiv: 0806.3603.
- [36] M. Notomi, E. Kuramochi, and T. Tanabe, *Nat. Photon.* **2**, 741 (2008).

Supplementary Material for “Photon Long-Range Repulsive Interaction in the Jaynes-Cummings Lattice with Rydberg Atoms”

I. Derivation of the Hamiltonian (1)

Figure S1(a) shows the system considered here: a one-dimensional cavity array coupled through photon hopping, with parameter κ [1], and an ensemble of Rydberg atoms placed in the center of each cavity. Figure S1(b) displays the energy-level structure of a single Rydberg atom. The single quantized cavity mode (i.e., photon), with annihilation operator a and frequency ω_c , induces a transition between the $5S_{1/2}$ ground state $|g\rangle$ and the $5P_{3/2}$ intermediate state $|p\rangle$, where the atom-photon interaction strength is determined by g_0 , while the other transition from the intermediate state $|p\rangle$ to the Rydberg state $|r\rangle$ is driven by a classical laser, with Rabi frequency Ω and driving frequency ω_l . Formally, the total Hamiltonian can be written as

$$H = H_{\text{JC}} + H_{\text{HOP}} + H_{\text{V}} - \mu N. \quad (\text{S6})$$

In the Hamiltonian (S6), H_{JC} describes the interaction between the photons and the ensemble of Rydberg atoms for all cavities. We first consider the interaction between the photon and a single three-level Rydberg atom at one cavity. In the rotating-wave approximation, the corresponding Hamiltonian is given by

$$H_1 = E_p |p\rangle \langle p| + E_r |r\rangle \langle r| + g_0(a^\dagger |g\rangle \langle p| + \text{H.c.}) + \omega_c a^\dagger a + [\Omega \exp(-i\omega_l t) |r\rangle \langle p| + \text{H.c.}], \quad (\text{S7})$$

where E_p and E_r are the energies of the intermediate state $|p\rangle$ and the Rydberg state $|r\rangle$, respectively. When the detuning is large, we can adiabatically eliminate the intermediate state $|p\rangle$, and rewrite the Hamiltonian (S7) via a unitary transformation as

$$H_2 = \omega a^\dagger a + \epsilon |r\rangle \langle r| + g_1(a^\dagger |g\rangle \langle r| + \text{H.c.}) + \lambda a^\dagger a |g\rangle \langle g|, \quad (\text{S8})$$

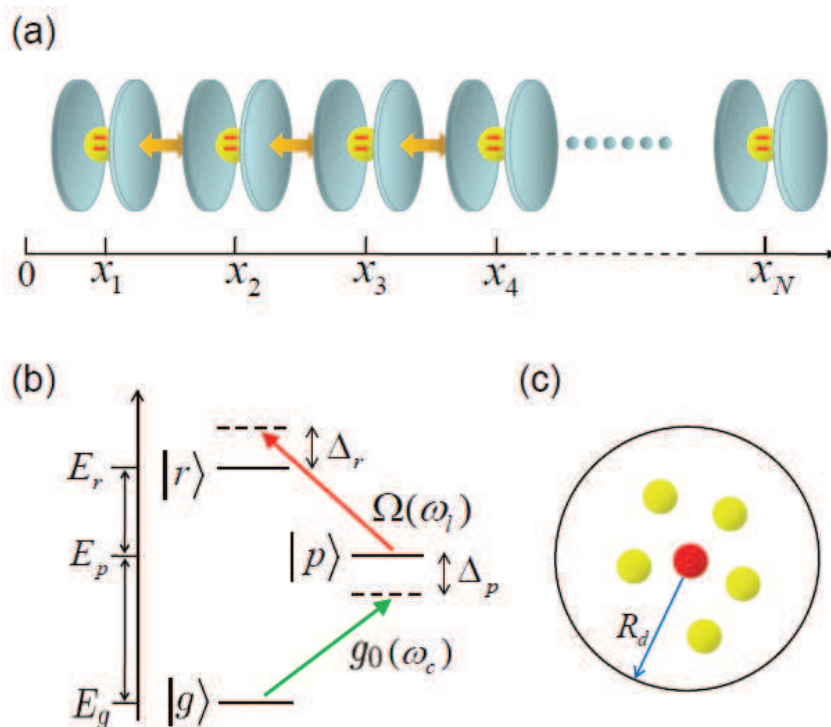


FIG. S1: (Color online) (a) Schematic diagram of a one-dimensional cavity array, with an ensemble of Rydberg atoms (yellow disks with two red levels) placed in the center of each cavity. Photons can hop between two adjacent cavities, indicated by orange double-arrows, due to the overlap of light modes. (b) Energy-level structure of a single three-level Rydberg atom, with detunings $\Delta_p = (E_p - E_g) - \omega_c$ and $\Delta_r = \omega_l - (E_r - E_p)$. (c) The strong van der Waals repulsive interaction make only one Rydberg atom excited in each cavity.

where $\omega = \omega_c - \omega_l$ is the effective photon frequency, $\epsilon = E_r - E_g - \omega_l + \Omega^2/\Delta_p$ is the effective transition frequency of the two-level Rydberg atom, $g_1 = g_0\Omega/\Delta_p$ is the effective interaction strength, and $\lambda = g_0^2/\Delta_p$. For large detuning, λ is very small and we thus can omit the interaction term $a^\dagger a |g\rangle \langle g|$.

In addition, for large detuning, g_1 is also weak. In order to enhance the effective atom-photon interaction strength, here we consider an ensemble of Rydberg atoms in the center of each cavity. For simplicity, we also assume that the number of Rydberg atoms in each cavity is a constant N_R . The strong van der Waals repulsive interaction between Rydberg atoms in the same cavity generates a Rydberg-blocked effect, with the blockade radius $R_d = 7 \mu\text{m}$ [4], which makes only one Rydberg atom excited; see Fig.S1(c). In such case, we should introduce the collective ground state $|G\rangle_i = |g_1, \dots, g_{N_R}\rangle_i$, and the collective excitation state $|R\rangle_i = \sum_f^{N_R} |r_f\rangle \langle g_f| \otimes |G\rangle_i / \sqrt{N_R}$. As a result, the first term of the Hamiltonian (S6) is given by

$$H_{\text{JC}} = \sum_i \left[\omega a_i^\dagger a_i + \epsilon |R\rangle_i \langle R|_i + g(a_i^\dagger |G\rangle_i \langle R|_i + \text{H.c.}) \right], \quad (\text{S9})$$

where the collective atom-photon interaction strength $g = \sqrt{N_R}g_0\Omega/\Delta_p = \sqrt{N_R}g_1$, and can reach the order of $\sim \text{MHz}$ [3, 4].

The second term in the Hamiltonian (S6) governs the photon hopping between two adjacent cavities, and is written as

$$H_{\text{HOP}} = -\kappa \sum_i (a_i^\dagger a_{i+1} + a_{i+1}^\dagger a_i), \quad (\text{S10})$$

where the hopping amplitude $\kappa = \omega_c/Q$, with Q being the quality factor of the cavity, and satisfying the condition $\kappa \leq g$. In order to achieve this condition, we require $Q \geq 10^6$, which has been realized experimentally in the large-scale ($L > 100$) array of the coupled nanocavities system [1].

The third term in the Hamiltonian (S6) governs the long-range van der Waals interaction between Rydberg atoms for different cavities, and is given by

$$H_{\text{V}} = \sum_{ij} \frac{V(i-j)}{2} |R\rangle_i \langle R|_i \otimes |R\rangle_j \langle R|_j, \quad (\text{S11})$$

where $V(i-j) = C_6/(x_i - x_j)^6$, with C_6 being the van der Waals coefficient and x_i being the position of the i th cavity. The long-range van der Waals interaction can induce a strong correlation between different sites. For example, if we choose $C_6 \approx 500 \text{ GHz}\cdot\mu\text{m}^6$ for the principal quantum number $n_P = 70$ [2] and $x_{i+1} - x_i \approx 0.7 \mu\text{m}$, the interaction between the 8th-neighbor sites, $V(8) \approx 2\pi \times 2.58 \text{ MHz}$ is still remarkable.

In the last term of the Hamiltonian (S6), the chemical potential μ is the Lagrange multiplier, and the total number of polaritons is given by $N = \sum_i n_i = \sum_i (a_i^\dagger a_i + |R\rangle_i \langle R|_i)$.

II. Derivation of the critical chemical potentials $\mu_\rho^0(p)$ and $\mu_\rho^0(h)$ for particles and holes

In the main text, we have described the low-energy behavior of the Hamiltonian (S6) by an effective Hamiltonian $H_{\text{eff}} = -J_\perp \sum_i \left(|\tilde{1}\rangle_i \langle 0|_i \otimes |0\rangle_{i+1} \langle \tilde{1}|_{i+1} + \text{H.c.} \right) + \sum_{ij} J_\parallel (i-j) |\tilde{1}\rangle_i \langle \tilde{1}|_i \otimes |\tilde{1}\rangle_j \langle \tilde{1}|_j / 2 + E_{1-}^\mu \sum_i |\tilde{1}\rangle_i \langle \tilde{1}|_i$. Moreover, we have also pointed out that when $J_\perp = 0$, there is a succession of photon crystal states with different filling factors, denoted as a photon devil's stair structure, and the energy gap of the photon crystal states can be calculated in terms of Eqs.(3) and (4) in the main text, i.e., $X_i^l = r_l$ or $r_l + 1$, and $\sum_i X_i^l = lN$. For example, we define the crystalline ground state, with the filling factor $\rho = p/q$, as $|c\rangle_q$. By adding one $|\tilde{1}\rangle$ state, the crystalline ground state $|c\rangle_q$ becomes $|p\rangle_q$. After rearranging the $|\tilde{1}\rangle$ states, the distance r_l between the $|\tilde{1}\rangle$ states is changed. Using Eqs.(3) and (4) in the main text, r_l $|\tilde{1}\rangle$ state pairs with $X_i^l = (r_l + 1)$ must be replaced by $(r_l + 1)$ $|\tilde{1}\rangle$ state pairs with $X_i^l = r_l$. So the corresponding energy shift, $\Delta E^+ = E(|p\rangle_q) - E(|c\rangle_q)$, is calculated as

$$\begin{aligned} \Delta E^+ &= E_{1-}^\mu + (r_1 + 1) J_\parallel(r_1) - r_1 J_\parallel(r_1 + 1) + (r_2 + 1) J_\parallel(r_2) - r_2 J_\parallel(r_2 + 1) + \dots \\ &\quad + q J_\parallel(q - 1) - (q - 1) J_\parallel(q) + \dots + 2q J_\parallel(2q - 1) - (2q - 1) J_\parallel(2q) + \dots, \end{aligned} \quad (\text{S12})$$

where $r_p = q, r_{2p} = 2q, \dots$, have been inserted [5]. Similarly, by removing one $|\tilde{1}\rangle$ state from $|c\rangle_q$, we obtain a new state $|h\rangle_q$. The corresponding energy shift, $\Delta E^- = E(|h\rangle_q) - E(|c\rangle_q)$, is calculated as

$$\begin{aligned} \Delta E^- &= -E_{1-}^\mu - (r_1 + 1) J_\parallel(r_1) + r_1 J_\parallel(r_1 + 1) - (r_2 + 1) J_\parallel(r_2) + r_2 J_\parallel(r_2 + 1) + \dots \\ &\quad - (q + 1) J_\parallel(q) + q J_\parallel(q + 1) - \dots - (2q + 1) J_\parallel(2q) + 2q J_\parallel(2q + 1) + \dots. \end{aligned} \quad (\text{S13})$$

These equations govern the energy gap of the photon crystal state $|c\rangle_q$. Obviously, at the phase-transition point, the energy gap is closed, i.e., $\Delta E^\pm = 0$. Using the expression $E_{1-}^\mu = (\omega - \mu) + \delta/2 - \sqrt{(\delta/2)^2 + g^2}$, we can derive the critical point of the chemical potential. The critical point between $|c\rangle_q$ and $|p\rangle_q$ is given by

$$\begin{aligned} \mu_\rho^0(p) &= \omega + \frac{\delta}{2} - \sqrt{\frac{\delta^2}{4} + g^2} \\ &+ \sum_{k=1, k \neq fp}^{\infty} [(r_k + 1) J_{\parallel}(r_k) - r_k J_{\parallel}(r_k + 1)] + \sum_{k=1}^{\infty} [kq J_{\parallel}(kq - 1) - (kq - 1) J_{\parallel}(kq)], \end{aligned} \quad (\text{S14})$$

where f is any integer. Similarly, the critical point between $|c\rangle_q$ and $|h\rangle_q$ is given by

$$\begin{aligned} \mu_\rho^0(h) &= \omega + \frac{\delta}{2} - \sqrt{\frac{\delta^2}{4} + g^2} \\ &+ \sum_{k=1, k \neq fp}^{\infty} [(r_k + 1) J_{\parallel}(r_k) - r_k J_{\parallel}(r_k + 1)] + \sum_{k=1}^{\infty} [(kq + 1) J_{\parallel}(kq) - kq J_{\parallel}(kq + 1)]. \end{aligned} \quad (\text{S15})$$

Using Eqs.(S14) and (S15), it is easy to evaluate the stability interval

$$\Delta\mu_\rho = \mu_\rho^0(p) - \mu_\rho^0(h) = \sum_{k=1}^{\infty} kq J_{\parallel}(kq + 1) + kq J_{\parallel}(kq - 1) - 2kq J_{\parallel}(kq). \quad (\text{S16})$$

From above discussions, we can see that there are infinity steps between any two states with different filling numbers. This means that there is a devil's-staircase structure of photon [5]. In addition, the expression for $\Delta\mu_\rho$ shows that the stability interval is only dependent on q , and moreover, decreases rapidly when increasing q . This indicates that the photon solid phases with $p = 1$, i.e., $\rho = 1/q = 1/2, 1/3, 1/4, \dots$, are more likely to be observed.

III. Derivation of Eq.(5)

We define

$$|\tilde{p}\rangle_q = \sum_{i=1}^{L/q} C_i |p\rangle_q^i \quad (\text{S17})$$

as a state with one particle-like defect, where the index i denotes the position of the defect and C_i is its coefficient. For simplicity, we only consider the lowest order of the photon hopping: the motion of the defect. Inserting $|\tilde{p}\rangle_q$ into equation $E(|\tilde{p}\rangle_q) |\tilde{p}\rangle_q = \langle \tilde{p} |_q H_{\text{eff}} | \tilde{p} \rangle_q$, we obtain

$$E(|\tilde{p}\rangle_q) = E^0(|\tilde{p}\rangle_q) - 2qJ_{\perp} \cos(\tilde{k}q), \quad (\text{S18})$$

where $E^0(|\tilde{p}\rangle_q)$ is the summation of the on-site and repulsive energies, $-2qJ_{\perp} \cos(\tilde{k}q)$ is the hopping energy band of a defect with wave number \tilde{k} . The phase boundary is determined by the lowest energy of $|\tilde{p}\rangle_q$, i.e., $\tilde{k} = 0$ and $E(|c\rangle_q) = E^0(|\tilde{p}\rangle_q) - 2qJ_{\perp}$. Thus, the upper bound of the photon solid phases is given by

$$\mu_\rho^{\text{up}} = \mu_\rho^0(p) - 2qJ_{\perp}. \quad (\text{S19})$$

Similar to the above discussions, the lower bound of the photon solid phases is obtained by

$$\mu_\rho^{\text{down}} = \mu_\rho^0(h) + 2qJ_{\perp}. \quad (\text{S20})$$

Equations (S19) and (S20) are the results in Eq.(5) of the main text.

* Corresponding author: chengang971@163.com

- [1] M. Notomi, E. Kuramochi, and T. Tanabe, *Nat. Photon.* **2**, 741 (2008).
- [2] H.P. Büchler, E. Demler, M. Lukin, A. Micheli, N. Prokofev, G. Pupillo, and P. Zoller, *Phys. Rev. Lett.* **98**, 0640404 (2007).
- [3] F. Brennecke, T. Donner, S. Ritter, T. Bourdel, M. Köhl, and T. Esslinger, *Nature (London)* **450**, 268 (2007).
- [4] C. Guerlin, E. Brion, T. Esslinger and K. Mølmer, *Phys. Rev. A* **82**, 053832 (2010).
- [5] P. Bak and R. Bruinsma, *Phys. Rev. Lett.* **49**, 249 (1982).